An Evaluation of MRI Safety and Compatibility of a Silver-Impregnated Antimicrobial Wound Dressing

John Nyenhuis, PhD, Lian Duan, MS

Purpose: Wound infections can slow healing, increase pain, and have negative effects on a patient's quality of life. The recent emergence of antibiotic-resistant bacterial strains has led wound care specialists to revisit alternative topical agents such as silver to control wound bioburden. Aquacel Ag is an ionic silver-containing barrier dressing that is able to absorb large amounts of wound exudate. The aim of this study was to assess the magnetic resonance (MR) safety and compatibility of this dressing, according to the standard requirements of the American Society for Testing and Materials (ASTM).

Methods: Radiofrequency-induced temperature changes associated with the test dressing were assessed using an ASTM phantom at 123 and 64 MHz. Whether the dressing caused any image distortion or magnetic deflection or if the electric resistance of the hydrated dressing differed significantly from that of tissue was also investigated.

Results: Similar radiofrequency-induced temperature changes were observed during 123 MHz (nominal 3 T) MR imaging of the phantom material alone (1.3°C) and when the dressing was added (1.8°C-2.0°C). Similar increases in temperature were also observed at 64 MHz (1.5 T) in the phantom material alone (1.4°C-1.9°C) and with the dressing (1.6°C-1.7°C). The test dressing did not cause any discernible image distortion or magnetic deflection and had similar electric resistance to human body tissues.

Conclusion: The wound dressing impregnated with ionic silver evaluated in this study has similar magnetic and electric characteristics to human tissues and is MR safe as defined in ASTM standard F2503-05. Therefore, the dressings can be left in place when a patient is undergoing MR imaging.

Key Words: Silver, antimicrobial, wound dressing, magnetic resonance imaging

J Am Coll Radiol 2009;6:500-505.

INTRODUCTION

The warm and moist wound environment is highly conducive to colonization by microorganisms [1], which can impede healing and lead to infection [2-4], even when the microbial load is relatively low [5]. Wound infection is known to increase pain and have detrimental effects on a patient's quality of life [5]. In light of these factors, the use of barrier dressings is important in the prevention of bacterial wound penetration [6].

The recent increase of antibiotic-resistant bacterial strains, particularly methicillin-resistant *Staphylococcus aureus* and vancomycin-resistant enterococci [1,3], as well as the shift toward reserving the use of antibiotics for the treatment of invasive infections [3,5], has emphasized the issue of appropriate wound care [5,7], particularly in cases in which blood flow to the wound is compromised [4,5]. This has led wound care specialists to revisit alternative topical agents such as silver to control wound bioburden [1,3,5,7].

Silver-containing dressing helps prevent infection by reducing the bioburden. Its use may reduce the need for antibiotics and thus reduce the incidence of antibiotic resistance. Silver impairs bacterial cell functionality by binding to, and inactivating, multiple enzymes and proteins in the cell membrane [7], and it has demonstrated antibacterial activity against a wide spectrum of pathogens [6]. The compound is also highly selective for bacterial cells, with even low concentrations leading to significant reductions in bacterial colonization, without causing host cell death [7]. The biocide mode of action of

School of Electrical and Computer Engineering, Purdue University, West Lafayette, Indiana.

Corresponding author and reprints: John A. Nyenhuis, PhD, Purdue University, School of Electrical and Computer Engineering, 465 Northwestern Avenue, West Lafayette, IN 47907-2035; e-mail: nyenhuis@ecn.purdue.edu.

This study was funded by ConvaTec (Skillman, NJ). Sushma Soni provided editorial assistance with support from ConvaTec.

0091-2182/09/$36.00 • DOI 10.1016/j.jacr.2009.02.013

silver makes the significant development of resistance unlikely [2], thus alleviating any concerns physicians may have regarding the overuse of silver-containing products [7]. Indeed, there is little published evidence to confirm the emergence of bacterial resistance to silver [2]. Furthermore, modern forms of silver delivery provide a sustained release of silver cations during their period of application, rather than an immediate "dose-dumping effect," as is seen with some dressing vehicles [6]. In this way, toxicity and buildup of pseudoeschar are avoided [1] while ensuring that silver is delivered to the wound in adequate therapeutic doses [4].

Aquacel Ag (ConvaTec, Skillman, New Jersey) is a dressing that contains ionic silver, which combines the antibacterial action of silver with a barrier dressing that utilizes Hydrofiber (E.R. Squibb & Sons, LLC, New Brunswick, New Jersey) technology (based on sodium carboxymethylcellulose) to absorb large amounts of wound exudate without requiring frequent dressing changes [3,6]. The dry fibers of the dressing form a gel when placed in contact with wound exudate, and the resulting swelling of the fibers locks the wound fluid, thereby containing bacteria away from the wound bed. Aquacel Ag has demonstrated excellent antibacterial properties against methicillin-resistant *S aureus* and vancomycin-resistant enterococci, as well as a wide range of anaerobic bacteria and yeasts frequently found in the wound bed, with microorganism cell death being observed within 30 minutes of exposure to the dressing [1,6].

Magnetic resonance (MR) and magnetic resonance imaging (MRI) is a medical imaging technique that can provide greater soft-tissue contrast than other imaging techniques, such as computed tomography. Furthermore, MRI does not use ionizing radiation, making it ideal for situations requiring multiple scans. Of relevance to the treatment of patients with thermal injury is the potential for the detection of soft-tissue infection on MRI [8].

Magnetic resonance imaging scanners generate powerful electromagnetic fields and use radiofrequencies (RFs) during image generation, which has implications for patients with certain indwelling metallic bodies (medical or otherwise) [9]. Issues include RF-induced heating of metallic objects, trauma due to movement of the objects, or device failure of the objects. In addition, such objects can result in image distortion. Patients with wounds may frequently require diagnostic imaging to ascertain the extent and progression of their injuries. Silver cations are known to possess some electrical conductivity [3] which may be of some concern for the use of MRI because the interaction of a conducting implant with the electric field induced by the RF magnetic field in MRI may result in excessive tissue heating.

We aimed in this study to assess the MR safety and compatibility of Aquacel Ag, according to the standard requirements of the American Society for Testing and Materials (ASTM) [10].

MATERIALS AND METHODS

Test Products

The products we tested in this study were commercially available 6 × 6-cm and 8 × 12-cm Aquacel Ag dressings and a 6 × 6-cm non-silver-containing Aquacel dressing. Silver cations were present at 1.2% of the total weight of the dressings [1].

RF-Induced Heating

The RF-induced heating of silver-containing test dressings was measured in vitro at 64 MHz (1.5 T) and at 123 MHz (2.9 T). We used a rectangular phantom similar to that described in ASTM standard F2182-02a [11]. Briefly, the phantom is a rectangular box comprising a "torso" portion measuring 42 × 60 cm and a "head" portion measuring 15 × 28 cm. The purpose of the phantom is to provide a test fixture to measure the heating of an implant in response to the electric field that is induced by the RF magnetic field in MRI. The overall procedure was done according to ASTM standard F2182-02a. The gelled saline phantom consisted of 8 g/L of poly(acrylic acid) (Aldrich Chemical, Milwaukee, Wisconsin) and 0.8 g/L of sodium chloride, with a conductivity of approximately 0.27 S/m and a depth of 12 cm. We measured the temperature increases induced by 15 minutes of exposure to the RF field using a Luxtron 790 fiber optic thermometry system (LumaSense Technologies, Santa Clara, California) with 0.6-mm-diameter small–form factor probes.

Figure 1 shows dressing and probe placement for the RF heating tests. In the measurements, the 6 × 6-cm silver-containing dressing was immersed in the phantom liquid near the side wall of the container, which is a region of high local specific absorption rate (SAR) because the SAR tends to be greatest at the periphery. The test dressing was suspended between two Teflon (DuPont, Wilmington, Delaware) posts on the holding grid and was folded to simulate the dressing being used to pack wound cavities. The thermometer probes were placed above the dressing, 4.5 cm from the wall of the phantom and were in contact with the dressing because of flotation. Before testing with a dressing, we first assessed RF-induced heating in the phantom in the absence of the test dressing to estimate background temperature increases. A reference probe was placed a distance away from the dressing, and the temperature increases at this probe location demonstrated that the RF power was consistently applied during the tests.

The temperature rise at 2.9 T (123 MHz) was measured in a Siemens whole-body MRI system (Siemens

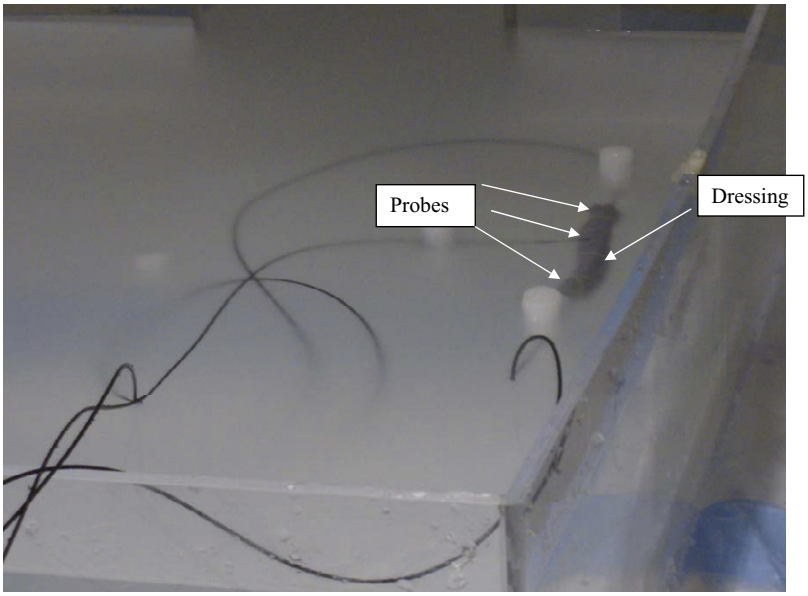

Fig 1. Close-up of dressing in gelled phantom near the side wall of the ASTM phantom container, indicating the thermometer probe locations for measurements of RF-induced temperature test product suspended in the gelled saline.

Medical Solutions, Erlangen, Germany) with a send-receive body coil at the Indiana University School of Medicine (Indianapolis, Indiana). The pulse sequence used was turbo spin-echo, with an echo time of 23 ms, a repetition time of approximately 500 ms, and a turbo factor of 7 and 4 slices. The flip angle was 180°, and the whole-body mean SAR, as reported by the console, was 3.1 W/kg. This sequence was chosen because it maximizes the SAR in the phantom, so that the measured temperature increases are "worst case." Temperature increases at 64 MHz were measured with a GE Signa whole-body RF coil (GE Healthcare, Milwaukee, Wisconsin). The RF magnetic field produced a continuous wave with a Wavetek model 3000 preamplifier (Willtek Communications GmbH, Ismaning, Germany) and an ENI power model 3200L amplifier (ENI, Rochester, New York). The phantom's average SAR in the measurements was approximately 2 W/kg. Although the continuous-wave RF field used for the 64-MHz tests is not suitable for imaging, it is appropriate for a heating study because the temperature increase of an implant will be proportional to the mean square value of the RF magnetic field. The RF magnetic field at both 64 and 123 MHz was circularly polarized.

Image Distortion

We assessed image distortion using the 2.9-T Siemens MRI system described above according to the protocol described in ASTM standard F2119-01, using MRI sequences defined therein [12]. These sequences were 1) spin echo with a repetition time of 500 ms and an echo time of 20 ms and 2) gradient echo with a repetition time of 100 ms, an echo time of 15 ms, and a flip angle of 30°. The phantom material we used consisted of 1.46 g/L sodium chloride and 1.5 g/L of hydrated copper sulfate. The same wadded silver-containing test dressing was used for the distortion tests as for the heating tests. Image distortion was not measured at 1.5 T because we expected that distortion at 2.9 T would be as great or greater than that at 1.5 T.

Magnetic Force Measurements

We assessed magnetic force using the 2.9-T Siemens Trio MR system. A dry, silver-containing test dressing was suspended by string at the edge of the bore. At this location, any magnetic force will be near the maximal value. The deflection angle was measured in accordance with protocols set out in ASTM standard F2052-02 [13].

Electric Resistance Measurements

Electrical measurements were made because the heating by the RF magnetic field in MRI depends on the electrical conductivity of an implant. To determine the conductivity of the dressing, we measured sheet resistance using the 4-point electrode method [14]. Two types of electrodes were used in testing: Euro cent and Silver Mactrode Plus electrocardiographic electrode (GE Healthcare). These electrodes have very different impedances; however, sheet resistance should be independent of this, and similar sheet-resistance values yielded by these two methods would demonstrate accuracy of the results. Figure 2 shows the setup for measurement of sheet resistance using the electrocardiographic electrodes. We soaked test dressings in tap water before the measurement of sheet resistance. A function generator was used to induce a current through the outer two electrodes, and the voltage between the inner two electrodes was measured with an oscilloscope.

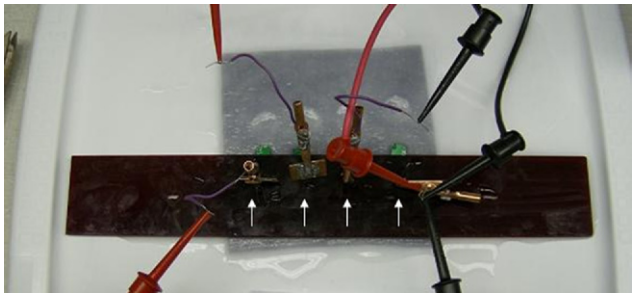

Fig 2. Four-point apparatus for measurement of sheet resistance of 6 × 6-cm silver dressing. Four electrocardiographic electrodes in a row are in contact with a hydrated dressing. White arrows indicate locations of electrodes.

RESULTS

RF-Induced Heating

Figure 3 shows the RF-induced rise at 123 MHz for one of the temperature probes in contact with the dressing. The linear rise in temperature vs time indicates that there was no site of intense local SAR near the dressing. The temperature increase vs time plot was also linear for the other heating measurements. The RF-induced temperature increases for the probes touching the dressing after 15 minutes of exposure are listed in Table 1. The mean increase of 1.87°C at 123 MHz compares with the background increase of 1.3°C. The greater increase with the dressing may be that, because of flotation, the dressing was about 2 cm higher in the phantom than was the probe during the background test. At 64 MHz (1.5 T), the mean RF-induced temperature increase was 1.7°C in both test and control experiments.

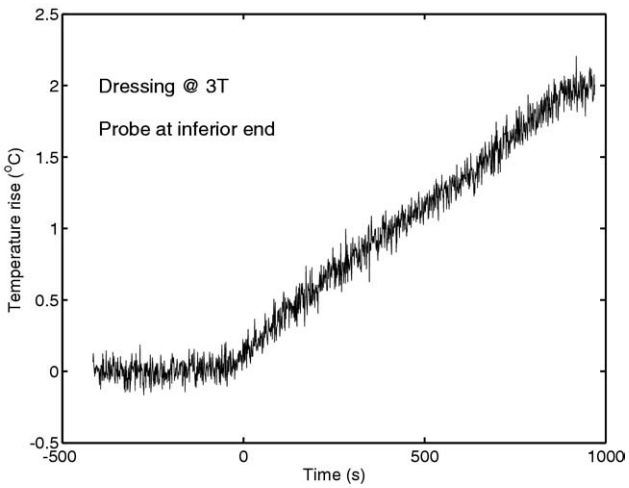

Fig 3. Temperature increase vs time for probe at inferior end of pad in Figure 1. The MRI scan starts at time = 0 s and ends at time = 900 s.

Table 1. Radiofrequency-induced temperature increases in the phantom material for the temperature probes in contact with the test product (6 × 6 cm)

Probe Location	ΔT With Dressing at 123 MHz	ΔT With Dressing at 64 MHz
Superior end of dressing	1.8°C	1.4°C
Center of dressing	2.0°C	1.9°C
Inferior end of dressing	1.8°C	1.9°C

Note: Probe locations are indicated in Figure 1; superior means that the probe was closer to the head end of the phantom. The background increase with no implant was 1.7°C at 64 MHz and 1.3°C at 123 MHz. The local background specific absorption rate for the 15 minutes of radiofrequency application was thus 7.9 W/kg at 64 MHz and 6.0 W/kg at 128 MHz.

Image Distortion

Figure 4 shows a spin-echo image from the image distortion test. The dressing appears dark on the MR image, indicating that the signal for the dressing was lower than that for the surrounding background. No discernible distortion was observed outside the dressing. Similarly, small distortion was exhibited for the gradient-echo image. If distortion existed, it did not extend beyond the 3-mm margin around the dressing. The box to the side of Figure 4 shows that the apparent size of the dressing was about 18 mm wide by 110 mm long. These dimensions are indistinguishable from the physical cross-section of the dressing.

Magnetic Force Testing

In magnetic force testing, no discernible deflection was observed when the suspended dressing was brought near the edge of bore of the 2.9-T Siemens MR system.

Electrical Measurements

Figure 5 shows the mean ± SD values for sheet resistance for 6 × 6-cm dressings with and without silver for frequencies from 0.1 to 20 kHz. In Figure 5, the low-frequency sheet resistance is approximately 1 kΩ/sq for the silvered dressing and 1.3 1 kΩ/sq for the non-silver-containing dressing. The range of measured sheet resistance measurements made with the electrocardiographic and Euro cent electrodes was 704 to 1700 Ω/sq. This range is felt to reflect the different measurement conditions (eg, extent of hydration of the dressings, nonuniformity in electrode spacings) and does not reflect intrinsic variation in the electrical properties of dressings.

The electrical conductivity σ of the hydrated dressing was calculated from the sheet resistance as follows:

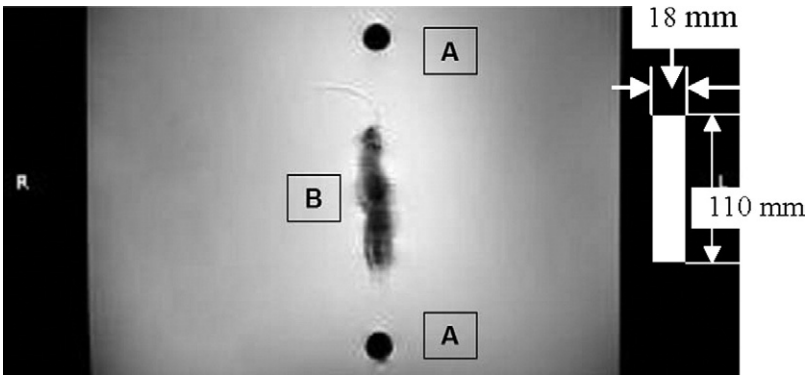

Fig 4. Coronal spin-echo image of the test dressing in the imaging phantom container. The dressing is indicated by B, and A indicates the Teflon posts from which the dressing is suspended. The white rectangle has dimensions of 18 × 110 mm, which are the approximate dimensions of the dark region in the image due to the dressing.

$$\sigma = 1/(R_s \times \text{thickness}). \quad (1)$$

Using a representative measured R_s value of 1000 Ω/sq and a gel thickness of 3 mm yields a conductivity of 0.33 S/m, which is within the range of the low-frequency conductivity for body tissues (about 0.5 S/m) [15]. Impedance measurements for test products were consistent with the measurements of sheet resistance (data not shown).

DISCUSSION

To the best of our knowledge, this is the first published study of the safety and compatibility of a silver-impregnated wound dressing in MRI. Patient safety in MR procedures is of paramount importance. Although the biologic effects of RF fields per se are considered minimal, MR procedures have resulted in some serious injuries, primarily as a result of the presence of metallic implants or devices [9]. Radiofrequency heating is a significant concern, with even some sporadic reports of skin irritation, cutaneous swelling, or heating sensation resulting from metallic pigments in skin tattoos and permanent cosmetics [9].

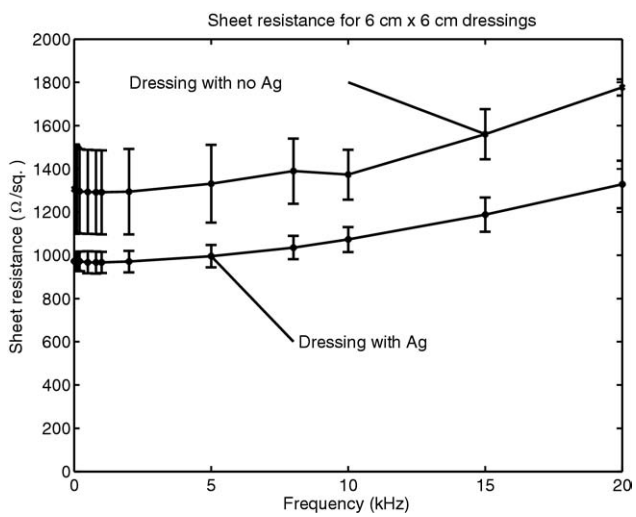

Fig 5. Measured sheet resistance for 6 × 6-cm dressings with and without silver. Data are presented as mean ± SD (n = 3).

The wound dressing evaluated in our study was associated with RF-induced temperature increases and electric resistance similar to those that would be expected in human tissue in the absence of a dressing. Also, the dressing exhibited no measurable magnetic force or torque. Thus, the dressing meets the ASTM standard F2503-05 requirements to be classified as MR safe in the MR environment [10]. The implication of our findings to clinical practice is that the silver dressing can remain in place while patients are undergoing diagnostic imaging, decreasing patient pain and distress and avoiding exposure of the wound and potential microbial colonization. Although the ASTM standard F2503-05 requirements do not extend to investigations of image artifacts, the test dressing did not seem to distort the image generated during MRI.

A number of different wound dressings and bandages containing silver are now available, with different compositions, levels of silver, and silver ion release rates [3], and all of these products indicate on their package inserts that the bandages should be removed before a patient undergoes MRI. However, the results presented here suggest that the wound dressing evaluated in our study is safe for use in MR equipment, in accordance with ASTM guidelines. This is most probably due to the low level of silver in the product that, nevertheless, has proven antimicrobial efficacy [1,6].

CONCLUSION

The ionic silver-containing wound dressing evaluated in our study has similar magnetic and electric properties to human tissues. The test results demonstrate that the dressing is safe for use in any MR environment and thus may be classified as MR safe as defined in ASTM standard F2503-05. The dressings can be left in place when a patient is undergoing imaging in any MR system. The image distortion tests indicate that the dressing will be

clearly imaged, although the MR signal produced by the dressing will depend on the specific pulse sequence and on the amount of absorbed exudate.

REFERENCES

1. Jones SA, Bowler PG, Walker M, Parsons D. Controlling wound bioburden with a novel silver-containing Hydrofiber dressing. Wound Repair Regen 2004;12:288-94.
2. Percival SL, Bowler PG, Russell D. Bacterial resistance to silver in wound care. J Hosp Infect 2005;60:1-7.
3. Tomaselli N. The role of topical silver preparations in wound healing. J Wound Ostomy Continence Nurs 2006;33:367-80.
4. Cutting KF. Wound healing, bacteria and topical therapies. EWMA J 2003;3:17-9.
5. Stephen-Haynes J, Toner L. Assessment and management of wound infection: the role of silver. Br J Commun Nurs 2007;12:S6-12.
6. Bowler PG, Jones SA, Walker M, Parsons D. Microbicidal properties of a silver-containing hydrofiber dressing against a variety of burn wound pathogens. J Burn Care Rehabil 2004;25:192-6.
7. Graham C. The role of silver in wound healing. Br J Nurs 2005;14:S22-26.
8. Miller TT, Randolph DA Jr, Staron RB, Feldman F, Cushin S. Fat-suppressed MRI of musculoskeletal infection: fast T2-weighted techniques versus gadolinium-enhanced T1-weighted images. Skeletal Radiol 1997;26:654-8.
9. Shellock FG, Crues JV. MR procedures: biologic effects, safety, and patient care. Radiology 2004;232:635-52.
10. American Society for Testing and Materials International. Standard practice for marking medical devices and other items for safety in the magnetic resonance environment. West Conshohocken, Pa: American Society for Testing and Materials International; 2005.
11. American Society for Testing and Materials International. Standard test method for measurement of radio frequency induced heating near passive implants during magnetic resonance imaging, standard F2182-02a. West Conshohocken, Pa: American Society for Testing and Materials International; 2002.
12. American Society for Testing and Materials International. Standard test method for evaluation of MR image artifacts from passive implants, standard F2119-01. West Conshohocken, Pa: American Society for Testing and Materials International; 2001.
13. American Society for Testing and Materials International. Standard test method for measurement of magnetically induced displacement force on medical devices in the magnetic resonance environment, standard F2052-02. West Conshohocken, Pa: American Society for Testing and Materials International; 2002.
14. Smits FM. Measurements of sheet resistivity with the four-point probe. Bell Syst Tech J 1958;37:371.
15. Italian National Research Council, Institute for Applied Physics. Dielectric properties of body tissues. Available at: http://niremf.ifac.cnr.it/tissprop/. Accessed April 28, 2009.